

Budgeted Training: Rethinking Deep Neural Network Training Under Resource Constraints

Mengtian Li[†]
Carnegie Mellon University

Ersin Yumer[†]
Uber ATG

Deva Ramanan
Carnegie Mellon University & Argo AI

Abstract

In most practical settings and theoretical analysis, one assumes that a model can be trained until convergence. However, the growing complexity of machine learning datasets and models may violate such assumptions. Moreover, current approaches for hyper-parameter tuning and neural architecture search tend to be limited by practical resource constraints. Therefore, we introduce a formal setting for studying training under the non-asymptotic, resource-constrained regime, i.e. budgeted training. We analyze the following problem: “given a dataset, algorithm, and resource budget, what is the best achievable performance?” We focus on the number of optimization iterations as the representative resource. Under such a setting, we show that it is critical to adjust the learning rate schedule according to the given budget. Among budget-aware learning schedules, we find simple linear decay to be both robust and high-performing. We support our claim through extensive experiments with state-of-the-art models on ImageNet (image classification), Cityscapes (semantic segmentation), MS COCO (object detection and instance segmentation), and Kinetics (video classification). We also analyze our results and find that the key to a good schedule is budgeted convergence, a phenomenon whereby the gradient vanishes at the end of each allowed budget. We also revisit existing approaches for fast convergence, and show that budget-aware learning schedules readily outperform such approaches under (the practical but under-explored) budgeted setting.

1. Introduction

Deep neural networks have made an undeniable impact in advancing the state-of-the-art for many fundamental computer vision tasks [27, 23, 8]. Much of these performance improvements were enabled by an ever-increasing amount of labeled data [50, 35, 29] and innovations in training architectures [34, 24].

However, as training datasets continue to grow in size,

[†]Work done while at Argo AI.

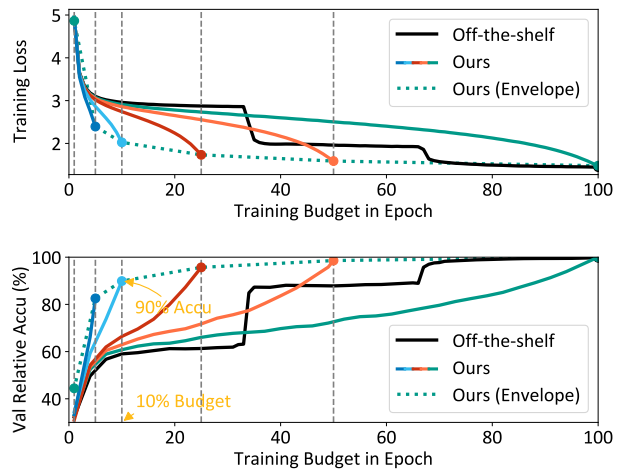


Figure 1. We formalize the intuitive but under-explored problem of *budgeted training*, in which one maximizes performance subject to a fixed number of training iterations. We find that a simple and effective solution is to adjust the learning rate schedule accordingly. This significantly outperforms off-the-shelf schedules, particularly for small budgets. This plot shows several training schemes (solid curves) for ResNet-18 [24] on ImageNet [50]. The vertical axis in the bottom plot is normalized by the validation accuracy achieved by the full budget training. The dotted green curve indicates an efficient way of trading off computation with performance.

we argue that an additional limiting factor is that of resource constraints for training. Conservative prognostications of dataset sizes – particularly for practical endeavours such as self-driving cars [2], assistive medical robots [58], and medical analysis [18] – suggest one will train on datasets orders of magnitude larger than those that are publicly available today. Such planning efforts will become more and more crucial, because *in the limit, it might not even be practical to visit every training example before running out of resources* [4, 46].

We note that resource-constrained training already is *implicitly* widespread, as the vast majority of practitioners have access to limited compute. This is particular true for those pursuing research directions that require a massive number of training runs, such as hyper-parameter tuning [36] and neural architecture search [71, 7, 38].

Instead of asking “what is the best performance one can achieve given this data and algorithm?”, which has been the primary focus in the field so far, we decorate this question with *budgeted training* constraints as follows: “what is the best performance one can achieve given this data and algorithm within the allowed budget?”. Here, the *allowed budget* refers to a limitation on total time, compute, or cost spent on training. More specifically, we focus on limiting the number of iterations. This allows us to abstract out the specific constraint without loss of generality since any one of the aforementioned constraints could be converted to a finite iteration limit. We make the underlying assumption that the network architecture is constant throughout training, though it may be interesting to entertain changes in architecture during training [51, 62].

Much of the theoretical analysis of optimization algorithms focuses on asymptotic convergence [49, 5, 42], which implicitly makes use of an *infinite* compute budget. In contrast, asymptotic convergence or global optimality is no longer the goal in the budgeted setting: rather, the question is how to maximize performance given the finite budget. This problem is not well-studied in theory nor understood in practice. Our work offers practical guidance for this setting, which is also suggestive of theoretical implications for deep learning optimization.

Given a limited budget, one obvious strategy might be data subsampling [1, 52, 63]. However, we discover that a much more effective but under-explored strategy is adopting budget-aware learning rate schedules — if we know that we are limited to a single epoch, one should tune the learning schedule accordingly. While this may seem obvious in retrospect, we specifically discover that a simple budget-aware strategy, that *linearly* decays the learning rate to 0, is more robust than complicated learning rate schedules suggested in prior work. Though we are motivated by budget-aware training, we find that a linear schedule is quite competitive for general learning settings as well. We verify our findings with state-of-the-art models on ImageNet (image classification), Cityscapes (semantic segmentation), MS COCO (object detection and instance segmentation), and Kinetics (video classification).

We conduct several diagnostic experiments that analyze learning rate decays under the budgeted setting. We first observe a statistical correlation between the learning rate and the *full* gradient magnitude (over the entire dataset). Decreasing the learning rate empirically results in a decrease of the full gradient magnitude. Eventually, as the former goes to zero, the latter vanishes as well, suggesting that the optimization has reached a critical point, if not a local minima¹. We call this phenomenon *budgeted convergence* and we find it generalizes across budgets. One one hand, it implies that

¹Whether such solution is exactly a local minimum or not is debatable (see Sec 3.1).

one should decay the learning rate to zero at the end of training, even given a small budget. On the other hand, it implies one should not aggressively decay the learning rate early in the optimization (such as the case with an exponential schedule) since this may slow down later progress. Finally, we show that linear budget-aware schedules outperform recently-proposed fast-converging methods that make use of adaptive learning rates and restarts.

Our main contributions are as follows:

- We introduce a formal setting for budgeted training based on training iterations and provide an alternative perspective for existing learning rate schedules.
- We discover that budget-aware schedules are handy solutions to budgeted training. Specifically, our proposed linear schedule is more simple, robust, and effective than prior approaches, for both budgeted and general training.
- We provide an empirical explanation to the heuristics of learning rate decay based on the correlation between learning rate and the full gradient norm.

2. Related Work

Learning rate schedule. A learning rate schedule is the set of *learning rates* or *step sizes* employed over the the entire course of the optimization. This important hyperparameter of deep networks is not well-studied in theory [69, 17, 16]. In practice, vision practitioners have developed several heuristic schedules for different purposes. For example, earlier image classification networks follow drop-on-plateau [34, 53, 24], newer ones adopt step decay [27, 67, 12, 60], while semantic segmentation tasks mostly use poly schedules [9, 70, 10, 11]. While these approaches adopt different schedules, the rationale is usually not discussed in depth. Such discussion can be found in dedicated work on proposing new learning rate schedules [39, 54, 25], but much of this past work limits their evaluation to CIFAR and ImageNet. For example, SGDR [39] advocates for learning-rate restarts based on the results on CIFAR, however, we find the unexplained form of cosine decay in SGDR is more effective than the restart technique. In our work, we rigorously evaluate on 5 standard vision benchmarks with state-of-the-art networks. A concurrent effort of [20] also analyzes learning rate restarts and in addition, the warm up technique, but does not analyze the specific form of learning rate decay.

Adaptive learning rate. Adaptive learning rate methods [59, 68, 30, 48] adjust the learning rate according to the local statistics of the cost surface. It is widely known that they produce inferior performance compared to SGD with momentum for benchmark tasks [64]. We examine this case by analyzing the equivalent learning rate. We find that the learning rate computed by these methods are too large for a budgeted convergence to take place.

3. Learning Rates and Budgets

In this section, we give a brief review of learning rates, then introduce our budget-aware setting, and conclude by proposing a linear-rate budget-aware schedule.

3.1. Learning Rates

A (stochastic) gradient descent update step is

$$w_t = w_{t-1} - \alpha_t g_t, \tag{1}$$

where t (from 1 to T) is the iteration, w are the parameters to be learned, g is the gradient estimator for the objective function F^2 , and α_t is the *learning rate*, also known as *step size*. Given base learning rate α_0 , we can define the ratio

$$\beta_t = \frac{\alpha_t}{\alpha_0}. \tag{2}$$

Then the set of $\{\beta_t\}_{t=1}^T$ is called the *learning rate schedule*, which specifies how the learning rate should vary over the course of training. Unlike prior art, our definition separates the base learning rate and learning rate schedule.

Learning rates are well studied for (strongly) convex cost surfaces. Constant learning rates are guaranteed to converge when less or equal than $1/L$, where L is the Lipschitz constant for the gradient of the cost function ∇F [5]. Another well-known result ensures convergence for sequences that decay neither too fast nor too slow [49]: $\sum_{t=1}^{\infty} \alpha_t = \infty, \sum_{t=1}^{\infty} \alpha_t^2 < \infty$. One common such instance in convex optimization is $\alpha_t = \alpha_0/t$. For non-convex problems, similar results hold for convergence to a local minimum [5]. Unfortunately, there does not exist a theory for learning rate schedules in the context of general non-convex optimization.

In deep learning, there is no consensus on the exact role of the learning rate. Most theoretical analysis makes the assumption of a small and constant learning rate [16, 17, 22]. For variable rates, one hypothesis is that large rates help move the optimization over large energy barriers while small rates help converge to a local minimum [26, 32, 39]. Such hypothesis is questioned by the recent mode connectivity analysis, which has revealed that there does exist a descent path between solutions that were previously thought to be isolated local minima [20, 19, 15]. Despite a lack of theoretical explanation, the community has adopted a variety of heuristic schedules for practical purposes, two of which are particularly common:

- **step decay:** drop the learning rate by a multiplicative factor γ after every d epochs. The default for γ is 0.1, but d varies significantly across tasks.

²Note that g can be based on a single example, a mini-batch, the full training set, or the true data distribution. In most practical settings, momentum SGD is used, but we omit the momentum here for simplicity.

- **exponential:** $\beta_t = \gamma^t$. There is no default parameter for γ and it requires manual tuning.

State-of-the-art codebases for standard vision benchmarks tend to employ step decay [27, 23, 8, 61, 66, 65, 40], whereas exponential decay has been successfully used to train Inception networks [56, 57, 55]. In spite of their prevalence, these heuristics have not been well studied.

3.2. Budget-Aware Schedules

Learning rate schedules are often defined assuming unlimited resources. As we argue, resource constraints are an undeniable practical aspect of learning. One simple approach for modifying an existing learning rate schedule to a budgeted setting is early-stopping. Fig 1 shows that one can dramatically improve results of early stopping by more than 60% by *tuning* the learning rate for the appropriate budget. To do so, we simply reparameterize the learning rate sequence with a quantity not only dependent on the absolute iteration t , but also the training budget T :

Definition (Budget-Aware Schedule). Let T be the training budget, t be the current step, then a training progress p is t/T . A *budget-aware learning rate schedule* is

$$\beta_p : p \mapsto f(p), \tag{3}$$

where $f(p)$ is the ratio of learning rate at step t to the base learning rate α_0 .

At first glance, it might be counter-intuitive for a schedule to *not* depend on T . For example, for a task that is usually trained with 200 epochs, training 2 epochs will end up at a solution very distant from the global optimal no matter the schedule. In such cases, conventional wisdom from convex optimization suggests that one should employ a large learning rate (constant schedule) that efficiently descends towards the global optimal. However, in the non-convex case, we observe empirically that a better strategy is to systematically decay the learning rate in proportion to the total iteration budget.

Budget-Aware Conversion (BAC). Given a particular rate schedule $\beta_t = f(t)$, one simple method for making it budget-aware is to rescale it, *i.e.*, $\beta_p = f(pT_0)$, where T_0 is the budget used for the original schedule. For instance, a step decay for 90 epochs with two drops at 30 epoch and 60 epoch will convert to a schedule that drops at 1/3 and 2/3 training progress. Analogously, an exponential schedule 0.99^t for 200 epochs will be converted into $(0.99^{200})^p$.

It is worth noting that such an adaptation strategy already exists in well-known codebases [23] for training with limited schedules. Our experiments confirm the effectiveness of BAC as a general strategy for converting many standard schedules to be budget-aware (Tab 1). *For our remaining experiments, we regard BAC as a known technique and apply it to our baselines by default.*

Budget	1%	5%	10%	25%	50%	100%
exp .99	.5848	.8030	.8352	.8888	.9072	.9320
BAC	.6086	.8560	.8996	.9228	.9272	N/A
step-d1	.5710	.8058	.8422	.8702	.8746	.9434
BAC	.5880	.8662	.9066	.9312	.9392	N/A

Table 1. Effectiveness of budget-aware conversion (BAC) on CIFAR-10 for image classification with ResNet-18 [24]. The numbers are classification accuracy on the validation set. The 100% budget refers to training for 200 epochs. “step-d1” denotes step decay dropping once at training progress 50%. Please refer to Sec 4.1 for the complete setup.

Recent schedules: Interestingly, several recent learning rate schedules are implicitly defined as a function of progress $p = \frac{t}{T}$, and so are budget-aware by our definition:

- **poly** [28]: $\beta_p = (1 - p)^\gamma$. No parameter other than $\gamma = 0.9$ is used in published work.
- **cosine** [39]: $\beta_p = \eta + \frac{1}{2}(1 - \eta)(1 + \cos(\pi p))$. η specifies a lower bound for the learning rate, which defaults to zero.
- **htd** [25]: $\beta_p = \eta + \frac{1}{2}(1 - \eta)(1 - \tanh(L + (U - L)p))$. Here η has the same representation as in cosine. It is reported that $L = -6$ and $U = 3$ performs the best.

The poly schedule is a feature in Caffe [28] and adopted by the semantic segmentation community [9, 70]. The cosine schedule is a byproduct in work that promotes learning rate restarts [39]. The htd schedule is recently proposed [25], which however, contains only limited empirical evaluation. None of these analyze their budget-aware property or provides intuition for such forms of decay. These schedules were treated as “yet another schedule”. However, our definition of budget-aware makes these schedules stand out as a general family.

3.3. Linear Schedule

Inspired by existing budget-aware schedules, we borrow an even simpler schedule from the simulated annealing literature [43, 31, 41]³:

$$\text{linear} : \beta_p = 1 - p. \quad (4)$$

To our best knowledge, a linear schedule that starts from the base learning rate and decays entirely to zero has not been used in major computer vision tasks. In Fig 2 (left), we compare linear schedule with various existing schedules under the budget-aware setting. Note that this linear schedule is completely parameter-free. This property is particularly desirable in budgeted training, where little budget

³A link between SGD and simulated annealing has been recognized decades ago, where learning rate plays the role of temperature control [3]. Therefore, cooling schedules in simulated annealing can be transferred into learning rate schedules for SGD.

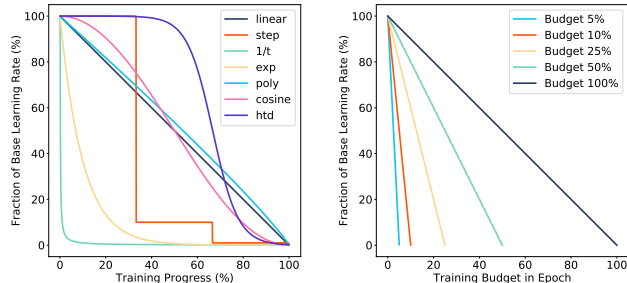


Figure 2. We normalize various learning rate schedules by training progress (left). Our solution to budgeted training is simple and universal — we decrease the learning rate linearly across the entire given budget (right).

exists for tuning such a parameter. The excellent generalization of linear schedule across budgets (shown in the next section) might imply that the cost surface of deep learning is to some degree self-similar. Note that a linear schedule, together with other recent budget-aware schedules, produces a constant learning rate in the asymptotic limit *i.e.*, $\lim_{T \rightarrow \infty} (1 - t/T) = 1$. Consequently, such practically high-performing schedules tend to be ignored in theoretical convergence analysis [49, 5].

4. Experiments

In this section, we first compare linear schedule against other existing schedules on the small CIFAR-10 dataset and then on a broad suite of vision benchmarks. The CIFAR-10 experiment is designed to extensively evaluate each learning schedule while the vision benchmarks are used to verify the observation on CIFAR-10. We provide important implementation settings in the main text while leaving the rest of the details to Appendix G. In addition, we provide in Appendix A & B the evaluation on a large number of random architectures in the setting of neural architecture search.

4.1. CIFAR

CIFAR-10 [33] is a dataset that contains 70,000 tiny images (32×32). Given its small size, it is widely used for validating novel ideas. We follow the standard setup for dataset split [27], which is randomly holding out 5,000 from the 50,000 training images to form the validation set. For each budget, we report the best validation accuracy among epochs up till the end of the budget. We use ResNet-18 [24] as the backbone architecture and utilize SGD with base learning rate 0.1, momentum 0.9, weight decay 0.0005 and a batch size 128.

We study learning schedules in several groups: (a) constant (equivalent to not using any schedule). (b) & (c) exponential and step decay, both of which are commonly adopted schedules. (d) htd [25], a quite recent addition and not yet adopted in practice. We take the parameters with the

Budget	1%	5%	10%	25%	50%	100%
const	.5830	.7968	.8410	.8662	.8726	.8790
exp .95	.4796	.7554	.8574	.9140	.9294	.9458
exp .97	.5546	.8222	.8556	.9112	.9456	.9552
exp .99	.6086	.8560	.8996	.9228	.9272	.9320
step-d1	.5806	.8648	.9066	.9318	.9408	.9434
step-d2	.5544	.8328	.9042	.9338	.9464	.9534
step-d3	.4882	.7942	.8872	.9260	.9436	.9532
htd	.6430	.8878	.9224	.9434	.9510	.9552
cosine	.6308	.8856	.9222	.9444	.9530	.9554
poly	.6584	.8912	.9244	.9416	.9494	.9534
linear	.6654	.8920	.9218	.9412	.9546	.9562

Table 2. Comparison of learning rate schedules on CIFAR-10. The 1st, 2nd and the 3rd place under each budget are color coded. The number here is the classification accuracy and each one is run 3 times independently and the median is taken. “step- d_x ” denotes decay x times at even intervals with $\gamma = 0.1$. For “exp” and “step” schedules, BAC (Sec 3.2) is applied in place of early stopping. We can see linear schedule surpasses other schedules under almost all budgets.

best reported performance $(-6, 3)$. Note that this schedule decays much slower initially than the linear schedule (Fig 2). (e) the smooth-decaying schedules (small curvature), which consists of cosine [39], poly [28] and the linear schedule.

As shown in Tab 2, the group of schedules that are budget-aware by our definition, outperform other schedules under all budgets. The linear schedule in particular, performs best most of the time including the typical full budget case. Noticeably, when exponential schedule is well-tuned for this task ($\gamma = 0.97$), it fails to generalize across budgets. In comparison, the budget-aware group does not require tuning but generalizes much better.

Within the budget-aware schedules, cosine, poly and linear achieve very similar results. This is expected due to the fact that their numerical similarity at each step (Fig 2). These results might indicate that *the key for a robust budgeted-schedule is to decay smoothly to zero*.

Based on these observations and results, we suggest linear schedule should be the “go-to” budget-aware schedule.

4.2. Vision Benchmarks

In the previous section we showed that linear schedule achieves excellent performance on CIFAR-10, in a relatively toy setting. In this section, we study the comparison and its generalization to practical large scale datasets with various state-of-the-art architectures. In particular, we set up experiments to validate the performance of linear schedule across tasks and budgets.

Ideally, one would like to see the performance of all

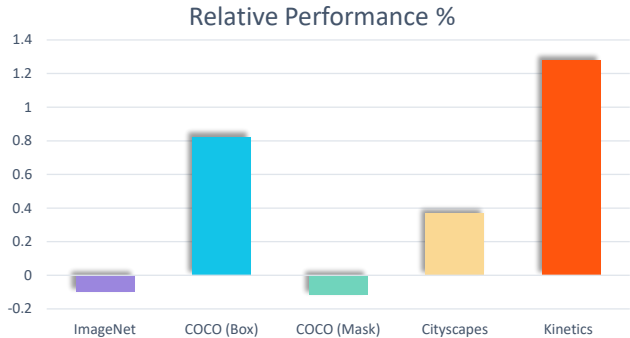


Figure 3. Robustness of linear schedule across tasks. Models solving standard vision benchmarks use different off-the-shelf schedules that are tuned for a particular configuration. But if we replace the off-the-shelf schedule with the simple linear schedule, instead of observing a significant performance drop, we observe comparable or even slightly better performance. See Tab 3 and Tab 4 for exact numbers.

schedules in Tab 2 on vision benchmarks. Due to resource constraints, we include only step decay, the off-the-shelf schedule if it is not step decay, and the linear schedule. Note our CIFAR-10 experiment suggests that using cosine and poly will achieve similar performance as linear, which are already budget-aware schedules given our definition, so we focus on linear schedule in this section.

We consider the following benchmarks covering the majority of fundamental vision problems:

Image classification on ImageNet. ImageNet [50] is a widely adopted standard for image classification task. The 2012-2017 version of the challenge contains more than 1 million Internet images covering 1k classes. We use ResNet-18 [24] and report the top-1 accuracy on the validation set with the best epoch. We follow the step decay schedule used in [27, 45], which drops twice at uniform interval. We set the full budget to 100 epochs (10 epochs longer than typical) for easier computation of the budget.

Object detection and instance segmentation on MS COCO. MS COCO [37] is a widely recognized benchmark for object detection and instance segmentation. The 2017 version of the challenge contains around 120k natural images for training and 5k for validation. We use the standard COCO AP (averaged over IoU thresholds) metric for evaluating bounding box output and instance mask output. The AP of the final model on the validation set is reported in our experiment. We use the challenge winner Mask R-CNN [23] with a ResNet-50 backbone and follows its setup. For training, we adopt the 1x schedule (90k iterations), and the off-the-shelf [23] step decay that drops 2 times with $\gamma = 0.1$ at $p \in [\frac{2}{3}, \frac{8}{9}]$. We train with 8 GPUs and keep the built-in learning rate warm up mechanism, which is an implementation technique that increases learning rate for 0.5k iterations and is intended for stabilizing the initial phase of multi-

Budget	1%	5%	10%	25%	50%	100%
Image classification on ImageNet with ResNet						
step	.2033	.5205	.5959	.6558	.6798	.6939
linear	.3080	.5721	.6231	.6632	.6812	.6932
Object detection on COCO with Mask-RCNN						
step	.0493	.2005	.2539	.3144	.3528	.3763
linear	.0514	.2092	.2627	.3215	.3574	.3794
Instance segmentation on COCO with Mask-RCNN						
step	.0487	.1926	.2392	.2906	.3198	.3399
linear	.0511	.1988	.2460	.2943	.3242	.3395
Semantic segmentation on Cityscapes with PSPNet						
step	.4944	.6332	.6796	.7242	.7465	.7646
linear	.5414	.6657	.7079	.7400	.7560	.7629
Video classification on Kinetics with I3D						
step	.2952	.4966	.5681	.6449	.6858	.7124
linear	.3296	.5304	.5964	.6638	.6998	.7215

Table 3. Robustness of linear schedule across budgets. Linear schedule significantly outperforms step decay given limited budgets. Note that the step decay used for each dataset is different, and it is the off-the-shelf schedule except for Cityscapes. For all step decay schedules, BAC (Sec 3.2) is applied to boost their budgeted performance. To reduce stochastic noise, we report the median of 3 independent runs for all the numbers. See Sec 4.2 for the metrics of each task.

Budget	1%	5%	10%	25%	50%	100%
poly	.5474	.6751	.7117	.7411	.7575	.7601
linear	.5414	.6657	.7079	.7400	.7560	.7629

Table 4. Comparison with off-the-shelf poly schedule on Cityscapes [14] using PSPNet [70]. Poly and linear are similar smooth-decaying schedules (Fig 2) and thus have similar performance. The exact rank differs from task to task. Same as above, the median of 3 runs is reported.

GPU training [21]. The 0.5k iterations are kept fixed for all budgets and learning rate decay is applied to the rest of the training progress.

Semantic segmentation on Cityscapes. Cityscapes [14] is a dataset commonly used for evaluating semantic segmentation algorithms. It contains high quality pixel-level annotations of 5k images in urban scenarios. The default evaluation metric is the mIoU (averaged across class) of the output segmentation map. We use state-of-the-art model PSPNet [70] with a ResNet-50 backbone and the full budget is 400 epochs as in standard set up. The mIoU of the best epoch is reported. Interestingly, unlike other tasks in this series, this model by default uses the poly [28] schedule. For complete evaluation, we also add a step decay that is the same in our ImageNet experiment.

Video classification on Kinetics with I3D. Kinetics [29] is a large-scale dataset of YouTube videos focusing on human actions. We use the 400-category version of the dataset and a variant of I3D [8] with training and data pro-

cessing code publicly available [61]. Top-1 accuracy of the final model is used for evaluating the performance. We follow the 4-GPU 300k iteration schedule [61], which features a step decay that drops 2 times with $\gamma = 0.1$ at $p \in [\frac{1}{2}, \frac{5}{6}]$.

Note that all off-the-shelf methods for these vision benchmarks employ SGD with momentum 0.9 and we adopt the same setting in our experiments.

First, we consider the full budget setting, where we simply swap out the off-the-shelf schedule with linear schedule. Fig 3 shows their relative performance and comparable or better performance is observed. This is surprising given the fact that linear schedule is parameter free. On the downside, this suggests that learning rate schedule is a unique hyper-parameter that is non-trivial to parameterize, or more specifically, to be optimized using grid search. Practical parameterization has not considered linear schedule as an option. On the upside, it shows that unlike other hyper-parameters, learning rate schedule does generalize across tasks and networks.

If we factor in the dimension of budgets, Tab 3 shows that the advantage of linear schedule over step decay becomes more obvious. For example, on ImageNet, linear achieves 51.5% improvement at 1% of the budget. In addition, we find linear schedule shares similar performance with the off-the-shelf poly schedule on Cityscapes (Tab 4). Given the similarity of poly and linear (Fig 2), and the opposite results on CIFAR-10 and Cityscapes, it is inconclusive that one is strictly better than the other within the smooth-decaying family.

In summary, *smoothly decaying budget-aware schedules, such as linear and poly, are simple and effective strategies for budgeted training.* They significantly outperform traditional step decay given limited budget, while achieving comparable performance with the normal full budget setting.

5. Discussion

In this section, we analyze what the *desiderata* of budget-aware learning schedules are. We also present findings that are inconsistent with conventional wisdom on aggressive descent and warm restarts. Note unless otherwise stated, the experiments in this section follow the setup in Sec 4.1.

Desideratum: budgeted convergence. Convergence of SGD under non-convex objectives is measured by $\lim_{t \rightarrow \infty} \mathbb{E}[\|\nabla F\|^2] = 0$ [5]. This is a desired property since if the SGD does not stop at a local minimum in the end, then it must be suboptimal. Intuitively, one might want to end the optimization in a location where further improvement cannot be easily made. If one is given a finite budget, a logical question to ask is: what is the counterpart for “convergence” within the budget?

For a dataset of N examples $\{(x_i, y_i)\}_{i=1}^N$, the full gra-

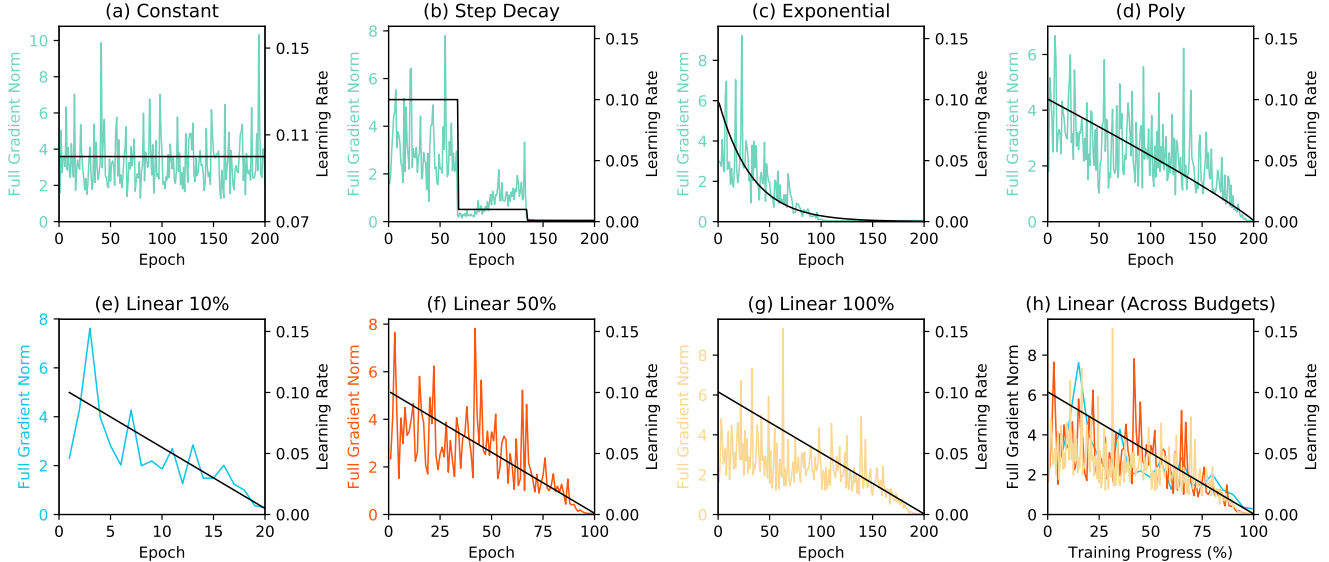


Figure 4. Budgeted convergence: full gradient norm $\|g_t^*\|$ vanishes over time (color curves) as learning rate α_t (black curves) decays. The first row shows that the dynamics of full gradient norm correlate with the corresponding learning rate schedule while the second row shows that such phenomena generalizes across budgets for budget-aware schedules. Such generalization is most obvious in plot (h), which overlays the full gradient norm across different budgets.

gradient $g_t^* = \frac{1}{N} \sum_{i=1}^N \nabla F(x_i, y_i)$. We find that the dynamics of $\|g_t^*\|$ over time highly correlates with the learning rate α_t (Fig 4). As learning rate vanishes for budget-aware schedules, the gradient magnitude $\|g_t^*\|$ also vanishes. We call this “vanishing gradient” phenomenon *budgeted convergence*. This could explain the rationale of why one should adjust schedules proportionally according to the budget. Specifically, one should have near zero learning rate at the end of the budget and use BAC instead of naive early stopping when the budget changes. For example, if we train with a budget-unaware exponential schedule for 50 epochs, from the third plot in Fig 4, the full gradient norm at that time is around 1.5, far above zero, suggesting this is a schedule with insufficient final decay of learning rate.

As a side note, our observation of budgeted convergence resonates with classic literature stating that SGD behaves like simulated annealing [3]. Since both α_t and $\|g_t^*\|$ are decreasing, $\|\alpha_t g_t^*\|$, the overall step size that SGD takes⁴, is also decreasing in expectation. In other words, large moves are more likely given large learning rates in the beginning, while small moves are more likely given small learning rates in the end. However, the exact mechanism is unclear of why gradient magnitude is influenced by learning rate irrespective of the optimization stage.

Desideratum: don’t waste budget. Fig 4 (b) shows that a step decay trained with 200 epochs reaches near zero gradient magnitude around epoch 150, shortly after the second drop. In addition, the validation accuracy (plot in Appendix

⁴Note that the momentum in SGD is used, but we assume vanilla SGD to simplify the discussion, without losing generality.

Schedule	Best Progress	Schedule	Best Progress
const	81.2% \pm 16.1%	step-d2	90.5% \pm 9.0%
linear	98.6% \pm 1.6%	poly	99.1% \pm 1.3%

Table 5. Where does one expect to find the model with the highest validation accuracy within the training progress? Here we show the best checkpoint location measured in training progress p and average for each schedule across budgets greater or equal than 10% and 3 different runs.

E) suggests that after epoch 150, the model is barely making any improvement. Together, these findings indicate that the budget after the second drop is not efficiently utilized. In contrast, the linear schedule makes small yet gradual and consistent improvement across the entire budget. Not only does the step decay make inefficient usage of the budget, but it also makes finding the best model harder. As a basic machine learning practise, one can validate the learned model using the validation set and report the checkpoint with the best accuracy. Tab 5 summarizes the location where the best model can be found on average. The step decay has the best location scattered out near the end of training while linear and poly can almost ensure the best model being at the very end. This is especially helpful for state-of-the-art models and complex problems, where evaluation can be very expensive due to the sheer size and the complicated metric (much more complicated than the loss itself). For example, validation takes several hours for video classification on Kinetics. With smooth-decaying budget-aware schedules, one only needs to validate the last few epochs to obtain the best model, thereby saving valuable compute budget at valida-

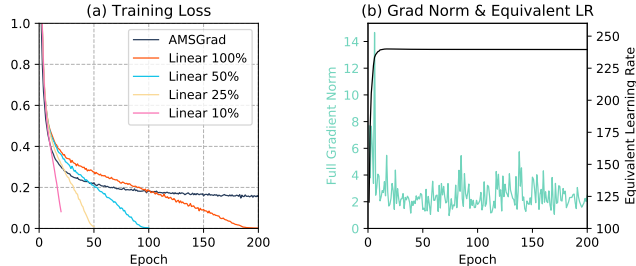


Figure 5. Comparing AMSGrad [48] with linear schedule. (a) while AMSGrad makes fast initial descent of the training loss, it is surpassed at each given budget by the linear schedule. (b) budgeted convergence is not observed for AMSGrad — the full gradient norm $\|g_t^*\|$ does not vanish (color curves). Comparing to a momentum SGD, AMSGrad recommends magnitudes larger learning rate $\tilde{\beta}_t$ (black curves).

tion time as well.

Validating faster optimization with budgeted training. Guided by asymptotic convergence analysis, faster descent of the objective might be an apparent desideratum of an optimization method. Many prior efforts claim their optimization methods to be superior based on a faster decrease of the objective [30, 48, 13]. Here we show that we need to rethink such claims in the deep learning world. Our budgeted training experiments on large vision benchmarks suggests that faster descent can be *trivially* and *universally* achieved by budget-aware schedules with a small budget. It is widely known that having a large learning rate usually leads to a faster descent, but it is less known that decaying the learning rate also achieves the same. Let us consider a faster descent baseline of AMSGrad [48], an adaptive learning rate method that fixes the convergence issue of the well-known optimizer Adam [30]. Adaptive learning rate methods try to estimate the local curvature information and accelerates training. However, as seen in Fig 5 (a), momentum SGD paired with linear schedule achieves a faster descent at each given budget. It is known that adaptive learning rates usually have a much worse empirical performance than well-tuned SGD [64], which is also evidenced by the fact that they are not adopted in standard vision benchmarks. Here we offer a possible explanation. In Fig 5 (b), the fluctuating gradient magnitude till the end shows that *AMSGrad does not converge under the budgeted setting*. Furthermore, we plot the equivalent learning rate $\tilde{\beta}_t$ relative to a momentum SGD with learning rate 0.1. Note that AMSGrad estimates a learning rate per each weight, and we take the median as a summary representation since it is a highly skewed distribution. Please refer to Appendix C for the exact derivation. This plot reveals that AMSGrad is using a far larger learning rate than momentum SGD, and does not vary according to the budget. Moreover, we find that forcing AMSGrad to decay by a companion decaying learning schedule improves validation accuracy (0.9113 to

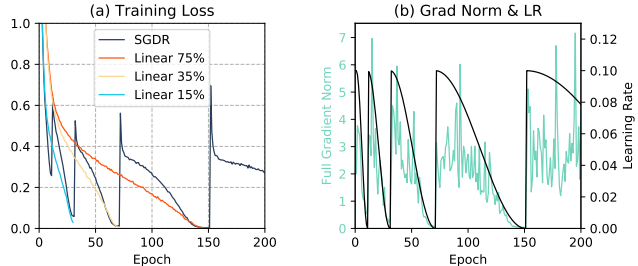


Figure 6. Comparing SGDR [39] with linear schedule. (a) SGDR makes slightly faster initial descent of the training loss, but is surpassed at each given budget by the linear schedule. (b) for SGDR, the correlation between full gradient norm $\|g_t^*\|$ and learning rate α_t is also observed. Warm restart does not help to achieve better budgeted performance.

0.9334), but still inferior to momentum SGD (0.9562), and such schedule is hard to tune for AMSGrad.

Anytime training and warm restart. A faster descent can also be interpreted from the perspective of anytime training. Anytime training considers the intermediate performance at all steps up till the budget, while budgeted training only considers the final performance. SGDR [39] has been proposed to improve the anytime performance. They used a periodical schedule, in which each period is a cosine schedule. They gave the intuition for this heuristics as escaping spurious local minima, which has been effectively questioned by [20]. Here we show that in Fig 6, similar to the results of AMSGrad showed earlier, SGDR has a fast descent, but inferior performance to budget-aware schedules at all given budgets. Additional comparison with SGDR can be found in Appendix D. Whether there exists a method that achieves promising anytime performance and budgeted performance at the same time remains an open question.

6. Conclusion

This paper introduces a formal setting for budgeted training. Under this setup, we observe that a simple linear schedule, or any other smooth-decaying schedules can achieve much better performance. Moreover, the linear schedule even offers comparable performance on existing visual recognition tasks for the typical full budget case. In addition, we analyze intriguing properties of learning rate schedule under budgeted training. We find that learning rate schedule controls the gradient magnitude regardless of training stage. This further suggests that SGD behaves like simulated annealing and the purpose of a learning rate schedule is to control the stage of optimization.

Acknowledgements: We thank Xiaofang Wang, Simon S. Du, Leonid Keselman, Chen-Hsuan Lin and David McAllester for insightful discussions and comments.

References

- [1] O. Bachem, M. Lucic, and A. Krause. Practical coresets constructions for machine learning. *arXiv preprint arXiv:1703.06476*, 2017. [2](#), [13](#)
- [2] M. Bojarski, D. D. Testa, D. Dworakowski, B. Firner, B. Flepp, P. Goyal, L. D. Jackel, M. P. Monfort, U. Muller, J. Zhang, X. Zhang, J. J. Zhao, and K. Zieba. End to end learning for self-driving cars. *CoRR*, abs/1604.07316, 2016. [1](#)
- [3] L. Bottou. Stochastic gradient learning in neural networks. In *Proceedings of Neuro-Nîmes 91*, Nîmes, France, 1991. EC2. [4](#), [7](#)
- [4] L. Bottou. Online algorithms and stochastic approximations. In D. Saad, editor, *Online Learning and Neural Networks*. Cambridge University Press, Cambridge, UK, 1998. revised, oct 2012. [1](#)
- [5] L. Bottou, F. E. Curtis, and J. Nocedal. Optimization methods for large-scale machine learning. *SIAM Review*, 60:223–311, 2018. [2](#), [3](#), [4](#), [6](#)
- [6] H. Cai, T. Chen, W. Zhang, Y. Yu, and J. Wang. Efficient architecture search by network transformation. In *AAAI*, 2018. [11](#)
- [7] S. Cao, X. Wang, and K. M. Kitani. Learnable embedding space for efficient neural architecture compression. *ICLR*, 2019. [1](#), [11](#)
- [8] J. Carreira and A. Zisserman. Quo vadis, action recognition? a new model and the kinetics dataset. *CVPR*, pages 4724–4733, 2017. [1](#), [3](#), [6](#)
- [9] L.-C. Chen, G. Papandreou, I. Kokkinos, K. Murphy, and A. L. Yuille. Deeplab: Semantic image segmentation with deep convolutional nets, atrous convolution, and fully connected crfs. *TPAMI*, 40:834–848, 2018. [2](#), [4](#)
- [10] L.-C. Chen, G. Papandreou, F. Schroff, and H. Adam. Rethinking atrous convolution for semantic image segmentation. *CoRR*, abs/1706.05587, 2017. [2](#)
- [11] L.-C. Chen, Y. Zhu, G. Papandreou, F. Schroff, and H. Adam. Encoder-decoder with atrous separable convolution for semantic image segmentation. In *ECCV*, 2018. [2](#)
- [12] Y. Chen, J. Li, H. Xiao, X. Jin, S. Yan, and J. Feng. Dual path networks. In *NIPS*, 2017. [2](#)
- [13] D.-A. Clevert, T. Unterthiner, and S. Hochreiter. Fast and accurate deep network learning by exponential linear units (elus). *ICLR*, 2016. [8](#)
- [14] M. Cordts, M. Omran, S. Ramos, T. Rehfeld, M. Enzweiler, R. Benenson, U. Franke, S. Roth, and B. Schiele. The cityscapes dataset for semantic urban scene understanding. In *CVPR*, 2016. [6](#)
- [15] F. Dräxler, K. Veschgini, M. Salmhofer, and F. A. Hamprecht. Essentially no barriers in neural network energy landscape. In *ICML*, 2018. [3](#)
- [16] S. S. Du, J. D. Lee, H. Li, L. Wang, and X. Zhai. Gradient descent finds global minima of deep neural networks. *arXiv preprint arXiv:1811.03804*, 2018. [2](#), [3](#)
- [17] S. S. Du, J. D. Lee, Y. Tian, B. Póczos, and A. Singh. Gradient descent learns one-hidden-layer cnn: Don’t be afraid of spurious local minima. In *ICML*, 2018. [2](#), [3](#)
- [18] M. Fatima and M. Pasha. Survey of machine learning algorithms for disease diagnostic. *Journal of Intelligent Learning Systems and Applications*, 9(01):1, 2017. [1](#)
- [19] T. Garipov, P. Izmailov, D. Podoprikin, D. P. Vetrov, and A. G. Wilson. Loss surfaces, mode connectivity, and fast ensembling of dnns. In *NeurIPS*, 2018. [3](#)
- [20] A. Gotmare, N. S. Keskar, C. Xiong, and R. Socher. A closer look at deep learning heuristics: Learning rate restarts, warmup and distillation. *ICLR*, 2019. [2](#), [3](#), [8](#)
- [21] P. Goyal, P. Dollár, R. Girshick, P. Noordhuis, L. Wesolowski, A. Kyrola, A. Tulloch, Y. Jia, and K. He. Accurate, large minibatch sgd: Training imagenet in 1 hour. *arXiv preprint arXiv:1706.02677*, 2017. [6](#)
- [22] M. Hardt, B. Recht, and Y. Singer. Train faster, generalize better: Stability of stochastic gradient descent. In *ICML*, 2016. [3](#)
- [23] K. He, G. Gkioxari, P. Dollár, and R. B. Girshick. Mask r-cnn. *ICCV*, pages 2980–2988, 2017. [1](#), [3](#), [5](#), [11](#)
- [24] K. He, X. Zhang, S. Ren, and J. Sun. Deep residual learning for image recognition. *CVPR*, pages 770–778, 2016. [1](#), [2](#), [4](#), [5](#)
- [25] B. Y. Hsueh, W. Li, and I.-C. Wu. Stochastic gradient descent with hyperbolic-tangent decay on classification. 2019. [2](#), [4](#)
- [26] G. Huang, Y. Li, G. Pleiss, Z. Liu, J. E. Hopcroft, and K. Q. Weinberger. Snapshot ensembles: Train 1, get m for free. *ICLR*, 2017. [3](#)
- [27] G. Huang, Z. Liu, L. van der Maaten, and K. Q. Weinberger. Densely connected convolutional networks. *CVPR*, pages 2261–2269, 2017. [1](#), [2](#), [3](#), [4](#), [5](#)
- [28] Y. Jia, E. Shelhamer, J. Donahue, S. Karayev, J. Long, R. Girshick, S. Guadarrama, and T. Darrell. Caffe: Convolutional architecture for fast feature embedding. In *Proceedings of the 22nd ACM international conference on Multimedia*, pages 675–678. ACM, 2014. [4](#), [5](#), [6](#)
- [29] W. Kay, J. Carreira, K. Simonyan, B. Zhang, C. Hillier, S. Vijayanarasimhan, F. Viola, T. Green, T. Back, A. Natsev, M. Suleyman, and A. Zisserman. The kinetics human action video dataset. *CoRR*, abs/1705.06950, 2017. [1](#), [6](#)
- [30] D. P. Kingma and J. Ba. Adam: A method for stochastic optimization. *ICLR*, 2015. [2](#), [8](#)
- [31] S. Kirkpatrick, C. D. Gelatt, and M. P. Vecchi. Optimization by simulated annealing. *science*, 220(4598):671–680, 1983. [4](#)
- [32] R. D. Kleinberg, Y. Li, and Y. Yuan. An alternative view: When does sgd escape local minima? In *ICML*, 2018. [3](#)
- [33] A. Krizhevsky and G. Hinton. Learning multiple layers of features from tiny images. Technical report, Citeseer, 2009. [4](#)
- [34] A. Krizhevsky, I. Sutskever, and G. E. Hinton. Imagenet classification with deep convolutional neural networks. *NIPS*, 60:84–90, 2012. [1](#), [2](#)
- [35] A. Kuznetsova, H. Rom, N. Alldrin, J. Uijlings, I. Krasin, J. Pont-Tuset, S. Kamali, S. Popov, M. Mallocci, T. Duerig, and V. Ferrari. The open images dataset v4: Unified image classification, object detection, and visual relationship detection at scale. *arXiv:1811.00982*, 2018. [1](#)

- [36] L. Li, K. G. Jamieson, G. DeSalvo, A. Rostamizadeh, and A. S. Talwalkar. Hyperband: A novel bandit-based approach to hyperparameter optimization. *Journal of Machine Learning Research*, 18:185:1–185:52, 2017. **1**
- [37] T.-Y. Lin, M. Maire, S. Belongie, J. Hays, P. Perona, D. Ramanan, P. Dollár, and C. L. Zitnick. Microsoft coco: Common objects in context. In *ECCV*, pages 740–755. Springer, 2014. **5**
- [38] H. Liu, K. Simonyan, and Y. Yang. Darts: Differentiable architecture search. *ICLR*, 2019. **1**
- [39] I. Loshchilov and F. Hutter. Sgdr: Stochastic gradient descent with warm restarts. 2016. **2, 3, 4, 5, 8, 12**
- [40] W. Ma, S. Wang, R. Hu, Y. Xiong, and R. Urtasun. Deep rigid instance scene flow. In *CVPR*, pages 1–9, 2019. **3**
- [41] D. McAllester, B. Selman, and H. Kautz. Evidence for invariants in local search. In *AAAI*, pages 321–326, 1997. **4**
- [42] A. Nemirovski, A. Juditsky, G. Lan, and A. Shapiro. Robust stochastic approximation approach to stochastic programming. *SIAM Journal on Optimization*, 19:1574–1609, 2009. **2**
- [43] Y. Nourani and B. Andresen. A comparison of simulated annealing cooling strategies. *Journal of Physics A: Mathematical and General*, 31(41):8373, 1998. **4**
- [44] H. Pham, M. Y. Guan, B. Zoph, Q. V. Le, and J. Dean. Efficient neural architecture search via parameter sharing. *ICML*, 2018. **11**
- [45] PyTorch. ImageNet training in PyTorch v1.0.1, 2019. Retrieved from <https://github.com/pytorch/examples/tree/master/imagenet> on Mar 4, 2019. **5**
- [46] P. Rai, H. Daumé, and S. Venkatasubramanian. Streamed learning: one-pass svms. In *Twenty-First International Joint Conference on Artificial Intelligence*, 2009. **1**
- [47] E. Real, A. Aggarwal, Y. Huang, and Q. V. Le. Regularized evolution for image classifier architecture search. *AAAI*, 2019. **11**
- [48] S. J. Reddi, S. Kale, and S. Kumar. On the convergence of adam and beyond. 2018. **2, 8, 12**
- [49] H. Robbins and S. Monro. A stochastic approximation method. *The annals of mathematical statistics*, pages 400–407, 1951. **2, 3, 4**
- [50] O. Russakovsky, J. Deng, H. Su, J. Krause, S. Satheesh, S. Ma, Z. Huang, A. Karpathy, A. Khosla, M. Bernstein, A. C. Berg, and L. Fei-Fei. ImageNet Large Scale Visual Recognition Challenge. *IJCV*, 115(3):211–252, 2015. **1, 5**
- [51] A. A. Rusu, N. C. Rabinowitz, G. Desjardins, H. Soyer, J. Kirkpatrick, K. Kavukcuoglu, R. Pascanu, and R. Hadsell. Progressive neural networks. *arXiv preprint arXiv:1606.04671*, 2016. **2**
- [52] O. Sener and S. Savarese. Active learning for convolutional neural networks: A core-set approach. *ICLR*, 2018. **2**
- [53] K. Simonyan and A. Zisserman. Very deep convolutional networks for large-scale image recognition. *ICLR*, 2015. **2**
- [54] L. N. Smith. Cyclical learning rates for training neural networks. *WACV*, pages 464–472, 2017. **2**
- [55] C. Szegedy, S. Ioffe, V. Vanhoucke, and A. A. Alemi. Inception-v4, inception-resnet and the impact of residual connections on learning. In *AAAI*, 2017. **3**
- [56] C. Szegedy, W. Liu, Y. Jia, P. Sermanet, S. Reed, D. Anguelov, D. Erhan, V. Vanhoucke, and A. Rabinovich. Going deeper with convolutions. In *CVPR*, pages 1–9, 2015. **3**
- [57] C. Szegedy, V. Vanhoucke, S. Ioffe, J. Shlens, and Z. Wojna. Rethinking the inception architecture for computer vision. In *CVPR*, pages 2818–2826, 2016. **3**
- [58] R. H. Taylor, A. Menciassi, G. Fichtinger, and P. Dario. Medical robotics and computer-integrated surgery. *Springer handbook of robotics*, pages 1199–1222, 2008. **1**
- [59] T. Tieleman and G. Hinton. RMSProp: Divide the gradient by a running average of its recent magnitude. *COURSERA: Neural Networks for Machine Learning*. **2**
- [60] F. Wang, M. Jiang, C. Qian, S. Yang, C. Li, H. Zhang, X. Wang, and X. Tang. Residual attention network for image classification. *CVPR*, pages 6450–6458, 2017. **2**
- [61] X. Wang, R. Girshick, A. Gupta, and K. He. Non-local neural networks. *CVPR*, 2018. **3, 6**
- [62] Y.-X. Wang, D. Ramanan, and M. Hebert. Growing a brain: Fine-tuning by increasing model capacity. In *Proceedings of the IEEE Conference on Computer Vision and Pattern Recognition*, pages 2471–2480, 2017. **2**
- [63] K. Wei, Y. Liu, K. Kirchhoff, and J. Bilmes. Using document summarization techniques for speech data subset selection. In *Proceedings of the 2013 Conference of the North American Chapter of the Association for Computational Linguistics: Human Language Technologies*, pages 721–726, 2013. **2**
- [64] A. C. Wilson, R. Roelofs, M. Stern, N. Srebro, and B. Recht. The marginal value of adaptive gradient methods in machine learning. In I. Guyon, U. V. Luxburg, S. Bengio, H. Wallach, R. Fergus, S. Vishwanathan, and R. Garnett, editors, *Advances in Neural Information Processing Systems 30*, pages 4148–4158. Curran Associates, Inc., 2017. **2, 8**
- [65] S. Xie and Z. Tu. Holistically-nested edge detection. In *ICCV*, 2015. **3**
- [66] Z. Yin, T. Darrell, and F. Yu. Hierarchical discrete distribution decomposition for match density estimation. *CVPR*, 2019. **3**
- [67] S. Zagoruyko and N. Komodakis. Wide residual networks. *BMVC*, 2016. **2**
- [68] M. D. Zeiler. Adadelta: An adaptive learning rate method. *CoRR*, abs/1212.5701, 2012. **2**
- [69] C. Zhang, S. Bengio, M. Hardt, B. Recht, and O. Vinyals. Understanding deep learning requires rethinking generalization. *ICLR*, 2017. **2**
- [70] H. Zhao, J. Shi, X. Qi, X. Wang, and J. Jia. Pyramid scene parsing network. *CVPR*, pages 6230–6239, 2017. **2, 4, 6**
- [71] B. Zoph and Q. V. Le. Neural architecture search with reinforcement learning. *ICLR*, 2017. **1, 11**

A. Rank Prediction for Neural Architecture Search

In the main text, we list neural architecture search as an application of budgeted training. Due to resource constraint, these methods usually train models with a small budget (10-25 epochs) to evaluate their relative performance [7, 6, 47]. Under this setting, *the goal is to rank the performance of different architectures* instead of obtaining the best possible accuracy as in the regular case of budgeted training. Then one could ask the question that whether budgeted training techniques help in better predicting the relative rank. Unfortunately, budgeted training has not been studied or discussed in the neural architecture search literature, it is unknown how well models only trained with 10 epochs can tell the relative performance of the same ones that are trained with 200 epochs. Here we conduct a controlled experiment and show that proper adjustment of learning schedule, specifically the linear schedule, indeed improves the accuracy of rank prediction.

We adapt the code in [7] to generate 100 random architectures, which are obtained by random modifications (adding skip connection, removing layer, changing filter numbers) on top of ResNet-18 [23]. First, we train these architectures on CIFAR-10 given full budget (200 epochs), following the setting described in Sec 4.1. This produces a relative rank between all pairs of random architectures based on the validation accuracy and this rank is considered as the target to predict given limited budget. Next, every random architecture is trained with various learning schedules under various small budgets. For each schedule and each budget, this generates a complete rank. We treat this rank as the prediction and compare it with the target full-budget rank. The metric we adopt is Kendall’s rank correlation coefficient (τ), a standard statistics metric for measuring rank similarity. It is based on counting the inversion pairs in the two ranks and $(\tau + 1)/2$ is approximately the probability of estimating the rank correctly for a pair.

We consider the following schedules: (1) constant, it might be possible that no learning rate schedule is required if only the relative performance is considered. (2) step decay ($\gamma = 0.1$, decay at $p \in [\frac{1}{3}, \frac{2}{3}]$), a schedule commonly used both in regular training and neural architecture search [71, 44]. (3) cosine, a schedule often used in neural architecture search [6, 47]. (4) linear, our proposed schedule. The results of their rank prediction capability can be seen in Tab 6.

The results suggest that with more budget, we can better estimate the full-budget rank between architectures. And even if only relative performance is considered, learning rate decay should be applied. Specifically, smooth-decaying schedule, such as linear or cosine, are preferred over step decay.

Epoch (Budget)	1 (0.5%)	2 (1%)	10 (5%)	20 (10%)
const	0.3451	0.4595	0.6720	0.6926
step-d2	0.2746	0.3847	0.6651	0.7279
cosine	0.3211	0.4847	0.7023	0.7563
linear	0.3409	0.4348	0.7398	0.7351

Table 6. Small-budget and full-budget model rank correlation measured in Kendall’s tau. Smooth-decaying schedules like linear and cosine can more accurately predict the true rank of different architectures given limited budget.

Epoch (Budget)	1 (0.5%)	2 (1%)	10 (5%)	20 (10%)
const	0.3892	0.4699	0.6689	0.7061
step-d2	0.4014	0.4780	0.6980	0.7754
cosine	0.4616	0.5498	0.7530	0.8029
linear	0.4759	0.5745	0.7652	0.8192

Table 7. Small-budget validation accuracy averaged across random architectures. Linear schedule is the most robust under small budgets.

Epoch (Budget)	1 (0.5%)	2 (1%)	10 (5%)	20 (10%)
const	0.4419	0.5343	0.7550	0.8015
step-d2	0.4590	0.5455	0.7894	0.8848
cosine	0.5326	0.6265	0.8615	0.9087
linear	0.5431	0.6626	0.8644	0.9305

Table 8. Tab 7 normalized by the full-budget accuracy and then averaged across architectures. Linear schedule achieves solutions closer to their full-budget performance than the rest of schedules under small budgets.

We list some additional details about the experiment. To reduce stochastic noise, each configuration under both the small and full budget is repeated 3 times and the median accuracy is taken. The full-budget model is trained with linear schedule, similar results are expected with other schedules as evidenced by the CIFAR-10 results in the main text (Tab 2). Among the 100 random architectures, 21 cannot be trained, the rest of 79 models have validation accuracy spanning from 0.37 to 0.94, with the distribution mass centered at 0.91. Such skewed and widespread distribution is the typical case in neural architecture search. We remove the 21 models that cannot be trained for our experiments. We take the epoch with the best validation accuracy for each configuration, so the drawback of constant or step decay not having the best model at the very end does not affect this experiment (see Sec 5).

B. Budgeted Performance Across Architectures

To reinforce our claim that linear schedule generalizes across different settings, we compare budgeted performance

of various schedules on random architectures generated in the previous section. We present two versions of the results. The first is to directly average the validation accuracy of different architecture with each schedule and under each budget (Tab 7). The second is to normalize by dividing the budgeted accuracy by the full-budget accuracy of the same architecture and then average across different architectures. The second version assumes all architectures enjoy equal weighting. Under both cases, linear schedule is the most robust schedule across architectures under various budgets.

C. Equivalent Learning Rate For AMSGrad

In Sec 5, we use equivalent learning rate to compare AMSGrad [48] with momentum SGD. Here we present the derivation for the equivalent learning rate $\tilde{\beta}_t$.

Let η_1, η_2 and ϵ be hyper-parameters, then the momentum SGD update rule is:

$$m_t = \eta_1 m_{t-1} + (1 - \eta_1) g_t, \quad (5)$$

$$w_t = w_{t-1} - \alpha_0^{(1)} \beta_t m_t, \quad (6)$$

while the AMSGrad update rule is:

$$m_t = \eta_1 m_{t-1} + (1 - \eta_1) g_t, \quad (7)$$

$$v_t = \eta_2 v_{t-1} + (1 - \eta_2) g_t^2, \quad (8)$$

$$\hat{m}_t = \frac{m_t}{1 - \eta_1^t}, \quad (9)$$

$$\hat{v}_t = \frac{v_t}{1 - \eta_2^t}, \quad (10)$$

$$\hat{v}_t^{\max} = \max(\hat{v}_t^{\max}, \hat{v}_t) \quad (11)$$

$$w_t = w_{t-1} - \alpha_0^{(2)} \frac{\hat{m}_t}{\sqrt{\hat{v}_t^{\max} + \epsilon}}. \quad (12)$$

Comparing equation 6 with 12, we obtain the equivalent learning rate:

$$\tilde{\beta}_t = \frac{\alpha_0^{(2)}}{\alpha_0^{(1)}} \frac{1}{(1 - \eta_1^t)(\sqrt{\hat{v}_t^{\max} + \epsilon})}, \quad (13)$$

Note that the above equation holds per each weight. For Fig 5, we take the median across all dimensions as a scalar summary since it is a skewed distribution. The mean appears to be even larger and shares the same trend as the median. In our experiments, we use the default hyper-parameters (which also turn out to have the best validation accuracy): $\alpha_0^{(1)} = 0.1, \alpha_0^{(2)} = 0.001, \eta_1 = 0.9, \eta_2 = 0.99$ and $\epsilon = 10^{-8}$.

D. Additional Comparison with SGDR

This section provides additional evaluation to show that learning rate restart produces worse results than our proposed budgeted training techniques under budgeted setting.

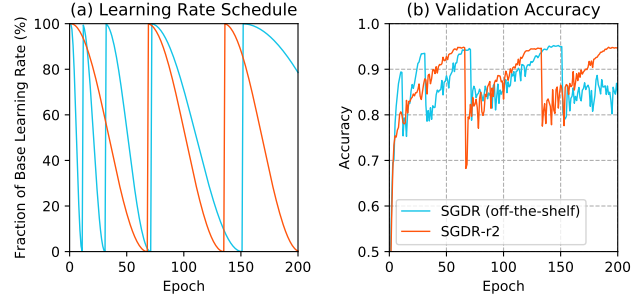


Figure 7. One issue with off-the-shelf SGDR ($T_0 = 10, T_{\text{mult}} = 2$) is that it is not budget-aware and might end at a poor solution. We convert it to a budget aware schedule by setting it to restart n times at even intervals across the budget and $n = 2$ is shown here (SGDR-r2).

Epoch	30	50	150
SGDR	.9320	.9458	.9510
linear	.9350	.9506	.9532

Table 9. Comparison with off-the-shelf SGDR at the end of each period after the first restart.

Budget	1%	5%	10%	25%	50%	100%
SGDR-r1	.5002	.7908	.8794	.9250	.9380	.9488
SGDR-r2	.4710	.7888	.8738	.9216	.9412	.9502
linear	.6654	.8920	.9218	.9412	.9546	.9562

Table 10. Comparison with SGDR under budget-aware setting. “SGDR-r1” refers to restarting learning rate once at midpoint of the training progress, and “SGDR-r2” refers to restarting twice at even interval.

In [39], both a new form of decay (cosine) and the technique of learning rate restart are proposed. To avoid confusion, we use “cosine schedule”, or just “cosine”, to refer to the form of decay and SGDR to a schedule of periodical cosine decays. The comparison with cosine schedule is already included in the main text. Here we focus on evaluating the periodical schedule. SGDR requires two parameters to specify the periods: T_0 , the length of the first period; T_{mult} , where i -th period has length $T_i = T_0 T_{\text{mult}}^{i-1}$. In Fig 7, we plot the off-the-shelf SGDR schedule with $T_0 = 10$ (epoch), $T_{\text{mult}} = 2$. The validation accuracy plot (on the right) shows that it might end at a very poor solution (0.8460) since it is not budget-aware. Therefore, we consider two settings to compare linear schedule with SGDR. The first is to compare only at the end of each period of SGDR, where budgeted convergence is observed. The second is to convert SGDR into a budget-aware schedule by setting the schedule to restart n times at even intervals across the budget. The results under the first and second setting is shown in Tab 9 and Tab 10 respectively. Under both budget-aware and budget-unaware setting, linear schedule outperforms SGDR. For

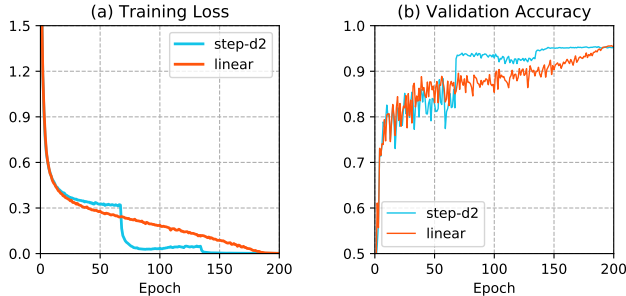


Figure 8. Training loss and validation accuracy for training ResNet-18 on CIFAR-10 using step decay and linear schedule. No generalization gap is observed when we only modify learning rate schedule. This figure provides details for the discussion of “don’t waste budget”.

detailed setup, we follow Sec 4.1, of the main text and take the median of 3 runs.

E. Additional Illustrations

In Sec 5, we refer to validation accuracy curve for training on CIFAR-10, which we provide here in Fig 8.

F. Data Subsampling

Data subsampling is a straight-forward strategy for budgeted training and can be realized in several different ways. In our work, we limit the number of iterations to meet the budget constraint and this effectively limits the number of data points seen during the training process. An alternative is to construct a subsampled dataset offline, but keep the same number of training iterations. Such construction can be done by random sampling, which might be the most effective strategy for *i.i.d*⁵ dataset. We show in Tab 11 that even our baseline budget-aware step decay, together with a limitation on the iterations, can significantly outperform this offline strategy. For the subset setting, we use the off-the-shelf step decay (step-d2) while for the full set setting, we use the same step decay but with BAC applied (Sec 3.2). For detailed setup, we follow Sec 4.1, of the main text and take the median of 3 runs.

Of course, more complicated subset construction methods exist, such as *core-set* construction [1]. However, such methods usually requires a feature summary of each data point and the computation of pairwise distance, making such methods unsuitable for extremely large dataset. In addition, note that our subsampling experiment is conducted on CIFAR-10, a well-constructed and balanced dataset, making smarter subsampling methods less advantageous. Consequently, the result in Tab 11 can as well provides a reasonable estimate for other complicated subsampling methods.

⁵independent and identically distributed

Budget	1%	5%	10%	25%	50%	100%
Subset	.3834	.6446	.7848	.8586	.9234	N/A
Full	.5544	.8328	.9042	.9338	.9464	.9534

Table 11. Comparison with offline data subsampling. “Subset” meets the budget constraint by randomly subsample the dataset prior to training, while “full” uses all the data, but restricting the number of iterations. Note that budget-aware schedule is used for “full”.

G. Additional Implementation Details

Image classification on ImageNet. We adapt both the network architecture (ResNet-18) and the data loader from the open source PyTorch ImageNet example⁶. The base learning rate used is 0.1 and weight decay 5×10^{-4} . We train using 4 GPUs with asynchronous batch normalization and batch size 128.

Object detection and instance segmentation on MS COCO. We use the open source implementation of Mask R-CNN⁷, which is a PyTorch re-implementation of the official codebase Detectron in the Caffe 2 framework. We only modify the part of the code for learning rate schedule. The codebase sets base learning rate to 0.02 and weight decay 10^{-4} . We train using 8 GPUs with asynchronous batch normalization and batch size 16.

Semantic segmentation on Cityscapes. We adapt a PyTorch codebase obtained from correspondence with the authors of PSPNet. The base learning rate is set to 0.01 with weight decay 10^{-4} . The training time augmentation includes random resize, crop, rotation, horizontal flip and Gaussian blur. We use patch-based testing time augmentation, which cuts the input image to patches of 713×713 and processes each patch independently and then tiles the patches to form a single output. For overlapped regions, the average logits of two patches are taken. We train using 4 GPUs with *synchronous* batch normalization and batch size 12.

Video classification on Kinetics with I3D. We use an open source codebase⁸ that has training and data processing code publicly available. Specifically, we follow the configuration of `run_i3d_baseline_300k_4gpu.sh`, which specifies a base learning rate 0.005 and a weight decay 10^{-4} . Only learning rate schedule is modified in our experiments. We train using 4 GPUs with asynchronous batch normalization and batch size 32.

⁶<https://github.com/pytorch/examples/tree/master/imagenet>. PyTorch version 0.4.1.

⁷<https://github.com/royseng-tw/Detectron.pytorch>. PyTorch version 0.4.1.

⁸<https://github.com/facebookresearch/video-nonlocal-net>. Caffe 2 version 0.8.1.